

# Input physical properties in mathematical model of steel quenching

**B. Smoljan\***, **D. Iljkić**, **L. Pomenić**

Department of Materials Science and Engineering,  
Faculty of Engineering, University of Rijeka,  
Vukovarska 58, HR-51000 Rijeka, Croatia

\* Corresponding e-mail address: smoljan@riteh.hr

Received 02.04.2013; published in revised form 01.06.2013

## Properties

### ABSTRACT

**Purpose:** Developing of new methods for input data of mathematical model is established.

**Design/methodology/approach:** Temperature dependency of both, heat transfer for quenchant with Grossmann severity of quenching  $H=0.35$ , which are adequate for oil and heat conductivity coefficients has been calibrated on the base of Crafts-Lamont diagrams.

**Findings:** Evaluation of physical properties such as specific heat capacity,  $c$ , heat conductivity coefficient,  $\lambda$ , density,  $\rho$ , heat transfer coefficient,  $\alpha$  involved in mathematical model of transient temperature field was done by the inversion method, or by calibrations.

**Research limitations/implications:** In the future this investigation should be broaden on investigation of more quenchants.

**Practical implications:** By proper input data of mathematical model of steel quenching, correct computer simulation can be performed.

**Originality/value:** New inverse method of input data such as specific heat capacity,  $c$ , heat conductivity coefficient,  $\lambda$ , density,  $\rho$ , heat transfer coefficient,  $\alpha$ , which is based just on achieved distributions of mechanical properties in Crafts-Lamont diagrams.

**Keywords:** Steel quenching; Numerical modelling; Hardness

**Reference to this paper should be given in the following way:**

B. Smoljan, D. Iljkić, L. Pomenić, Input physical properties in mathematical model of steel quenching, Journal of Achievements in Materials and Manufacturing Engineering 58/2 (2013) 81-86.

## 1. Introduction

Simulation of steel quenching is a complex problem. Research of numerical simulation of hardening degree distribution in quenched steel specimen is one of the highest priority researches in simulation of phenomena of steel quenching [1-6].

Generally the mathematical modelling of steel quenching can be divided in two parts, numerical simulation of specimen cooling and numerical simulation of specimen hardening. Rate of steel specimen cooling essentially depends on specimen geometry and characteristic physical properties of quenchant and quenched steel. Main physical properties about which cooling rate depends

are specific heat capacity of steel, heat conductivity coefficient of steel, steel density, heat transfer coefficient of quenchant. For precise mathematical modelling these variables must be estimated with high precision. These variables can be predicted experimentally for the concrete quenchant and steel [7]. Experimentally evaluated variables are successfully applicable only for particular steel and quenchant used at experiment.

Another way of estimating of data involved in mathematical model of transient temperature field can be done by inversion method based on relation between cooling curves and heat conductivity coefficients [7, 8]. More generally applied method of estimation of needed physical properties for modelling of quenching is method based on achieved results and qualitative

analysis of cooling curve. In this way physical properties are adjusted or calibrated with the results of quenching. Physical properties predicted by this method are usable for large spectra of quenchants with the same intensity of cooling, and for large spectra of steels [9].

## 2. Mathematical modelling of cooling

The temperature field change in an isotropic rigid body without heat sources can be described by Fourier's law of heat conduction:

$$\frac{\delta(c\rho T)}{\delta t} = \text{div} \lambda \text{grad} T \tag{1}$$

where  $\lambda/\text{Wm}^{-1}\text{K}^{-1}$  is the coefficient of heat conductivity,  $\rho/\text{kgm}^{-3}$  is the density,  $c/\text{Jkg}^{-1}\text{K}^{-1}$  is the specific heat capacity.

Characteristic initial condition is:

$$-\lambda \frac{\delta T}{\delta n} \Big|_s = \alpha(T_s - T_f) \tag{2}$$

where  $T_s/\text{K}$  is the surface temperature,  $T_f/\text{K}$  is the quenchant temperature,  $\alpha/\text{Wm}^{-2}\text{K}^{-1}$  is the heat transfer coefficient.

Solution of equation (1) can be found out using the finite volume method [10,11]. Transient temperature field in an isotropic rigid body can be defined by 2-D finite volume formulation (Fig. 1):

$$\begin{aligned} T_{ij}^1 \left( \sum_{m=1}^2 b_{1(i+n)j} + \sum_{m=1}^2 b_{ji(j+n)} + b_{ij} \right) &= \\ &= \sum_{m=1}^2 \left( b_{1(i+n)j} T_{i+k}^1 + b_{ji(j+n)} T_{i(j+k)}^1 \right) + b_{ij} T_{ij}^0 \end{aligned} \tag{3}$$

$$i = 1, 2, \dots, i_{\max}, \quad j = 1, 2, \dots, j_{\max}, \quad n = 2 - m, \quad k = 3 - 2m$$

where  $T_{ij}^0/\text{K}$  is the temperature in the beginning of time step  $\Delta t$ ,  $T_{ij}^1/\text{K}$  is the temperature in the end of time step  $\Delta t$ ,  $\Delta t/s$  is the time step,  $b_{ij} = (\rho_j c_{ij} \Delta V_{ij})/\Delta t$ ,  $\Delta V_{ij}/\text{m}^3$  is the volume of the control volume,  $b_{1(i+n)j} = W_{1(i+n)j}^{-1}$  and  $b_{ji(j+n)} = W_{ji(j+n)}^{-1}$ , where variables  $W_{1(i+n)j}$  and  $W_{ji(j+n)}$  are the thermal resistances between  $ij$  and  $(i+k)j$  volume and between  $ij$  and  $i(j+k)$  volume.

$$W_{1(i+n)j} = \frac{1}{\Delta F_{1(i+n)j}} \left( \frac{l_{ijm}}{\lambda_{ij}} + \frac{l_{1(i+k)j(3-m)}}{\lambda_{1(i+k)j}} \right) \tag{4}$$

$$W_{ji(j+n)} = \frac{1}{\Delta F_{ji(j+n)}} \left( \frac{l_{ijm}}{\lambda_{ij}} + \frac{l_{i(j+k)(3-m)}}{\lambda_{i(j+k)}} \right) \tag{5}$$

Thermal resistances for boundary volume are:

$$W_{1(i+n)j} = \frac{1}{\Delta F_{1(i+n)j}} \left( \frac{l_{ij}}{\lambda_{ij}} + \frac{1}{\alpha_{\text{Ts}1(i+n)j} \cos \varphi_{1(i+n)j}} \right) \tag{6}$$

$$W_{ji(j+n)} = \frac{1}{\Delta F_{ji(j+n)}} \left( \frac{l_{ij}}{\lambda_{ij}} + \frac{1}{\alpha_{\text{Ts}ji(j+n)} \cos \varphi_{ji(j+n)}} \right) \tag{7}$$

where  $\alpha_{\text{Ts}}/\text{Wm}^{-2}\text{K}^{-1}$  is the heat transfer coefficient at the boundary temperature  $T_s$ , and  $\cos \varphi$  is the direction cosines of heat flux.

Discretization system has  $N$  linear algebraic equations with  $N$  unknown temperatures of control volumes, where  $N$  is total number of control volumes. Time of cooling from  $T_a$  to specific temperature in particular point is determined as sum of time steps, and in this way, the diagram of cooling curve in every grid-point of a specimen is possible to found out.

$$t_M = \sum_{m=1}^M \Delta t_m \tag{8}$$

where  $M$  is the number of time steps during the cooling from 800 to 500°C.

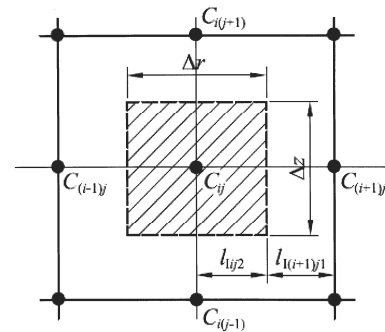


Fig. 1. Control volume

Before setting of model of temperature field change in an isotropic rigid body input data, i.e., specific heat capacity of steel,  $c$ , heat conductivity coefficient of steel,  $\lambda$ , steel density,  $\rho$ , heat transfer coefficient of quenchant,  $\alpha$  must be consistent with the achieved results of microstructure and mechanical properties. Optimization of input data should be done according to achieved results.

## 3. The calibration of input data involved in mathematical model of transient temperature field

Variable  $\rho$  for steel is equal  $\sim 7800 \text{ kgm}^{-3}$ . Accepted values of specific heat capacity,  $c$  are shown in Table 1 [12].

If the variables  $\rho$  and  $c$  were accepted, variable  $\lambda$  and specially variable  $\alpha$  must be estimated, i.e., calibrated according to variables  $\rho$  and  $c$ .

The input values of heat transfer coefficient have been optimized using *Crafts-Lamont* diagrams. Optimization was done for large spectra of a specimen bar diameter. Estimation of heat transfer coefficient was provided by varying of heat transfer coefficient values in the established model of cooling of steel bar.

Table 1.  
Accepted values of specific heat capacity

Specific heat capacity, $c/(J/kgK)$	Temperature, Ferrite + Pearlite (Bainite)		Martensite	Austenite
	$T/^\circ C$			
	0	378	376	415
	300	446	445	440
	600	509	507	467
	800	570	-	490
	950	596	-	520

Table 2.  
Calibrated values of heat transfer coefficient

Temperature, $T/^\circ C$	19.5	322	415	553	950
Heat transfer coefficient, $\alpha/Wm^{-2}K^{-1}$	498	645	1533	829	696

For different *Grossmann* severity of quenching and different bar diameters the cooling time from 800 to 500°C was calculated in different distance from bar surface. After that the distance from a quenched end of *Jominy* specimen was estimated using a relation which exists between cooling time from 800 to 500°C and distance from a quenched end of *Jominy* specimen (Fig. 2) [13].

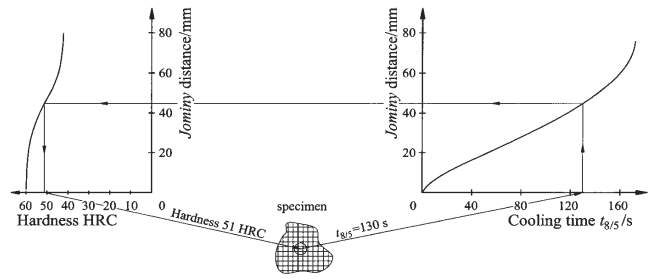


Fig. 2. Conversion of the cooling time  $t_{8/5}$  to the hardness

Calculated values of distances from a quenched end of *Jominy* specimen have been compared with those evaluated by *Crafts-Lamont* diagrams.

Temperature field change of specimen was calculated for radius position  $r/R=0$ ,  $r/R=0.5$  and  $r/R=0.9$ . Relative differences between distance from a quenched end of *Jominy* specimen estimated by modelling and by *Crafts-Lamont* diagrams were negligible, relative errors were less than 10%. Calibrated values of heat transfer coefficient,  $\alpha$  for *Grossmann* severity of quenching  $H=0.35$  are presented in Table 2.

Table 3.  
Regression relations between heat conductivity coefficients and hardenability properties

Microstructure	Temperature, $T/^\circ C$	Heat conductivity coefficients/(W/mK)
Ferrite + Pearlite (Bainite)	20	$\lambda_{(F+P)20} = \lambda_{B20} = 63 - 0.29HRC_{max} - 9 \frac{E_d}{HRC_{max} - 20}$ (9a)
	300	$\lambda_{(F+P)300} = \lambda_{B300} = 51 - 0.14HRC_{max} - 4.8 \frac{E_d}{HRC_{max} - 20}$ (9b)
	500	$\lambda_{(F+P)500} = \lambda_{B500} = 42 - 0.08HRC_{max} - 2.4 \frac{E_d}{HRC_{max} - 20}$ (9c)
	800	$\lambda_{(F+P)800} = \lambda_{B800} = 31 - 0.02HRC_{max} - 1.2 \frac{E_d}{HRC_{max} - 20}$ (9d)
Martensite	20	$\lambda_{M20} = 63 - 0.29HRC_{max} - 9 \frac{E_d}{HRC_{max} - 20}$ (10a)
	300	$\lambda_{M300} = 45 - 0.13HRC_{max} - 4.3 \frac{E_d}{HRC_{max} - 20}$ (10b)
	500	$\lambda_{M500} = 37 - 0.07HRC_{max} - 2.2 \frac{E_d}{HRC_{max} - 20}$ (10c)
Austenite	20	$\lambda_{A20} = 19 - 0.09HRC_{max} - 2.8 \frac{E_d}{HRC_{max} - 20}$ (11a)
	300	$\lambda_{A300} = 22 - 0.06HRC_{max} - 2.1 \frac{E_d}{HRC_{max} - 20}$ (11b)
	500	$\lambda_{A500} = 26 - 0.05HRC_{max} - 1.6 \frac{E_d}{HRC_{max} - 20}$ (11c)
	800	$\lambda_{A800} = 29 - 0.02HRC_{max} - 1.1 \frac{E_d}{HRC_{max} - 20}$ (11d)

Simultaneously with estimation of heat transfer coefficient for different *Grossmann* severity of quenching, heat conductivity coefficients have been estimated.

Regression relations between heat conductivity coefficients for different temperature and hardenability properties are expressed by the equations (9), (10) and (11) in Table 3. In Table 3  $HRC_{max}$  is maximum hardness in *Jominy* curve, and  $E_d$  is distance from a quenched end of *Jominy* specimen with 50% of martensite in the microstructure. Distance  $E_d$  was estimated by the *Jominy* curve based on hardness of steel with 50% of martensite in the microstructure. Hardness of steel with 50% of martensite in the microstructure was calculated by:

$$HRC_{M50} = 0.73HRC_{max} \tag{12}$$

Temperature, $T$	$T_8$	100%A	100%A	100%A	100%A	100%A	100%A	100%A	100%A	100%A	100%A	100%A
	$T_7$	100%A	100%A	100%A	100%A	100%A	100%A	100%A	87.5%A 12.5%F	75%A 25%F		
	$T_6$	100%A	100%A	100%A	100%A	100%A	100%A	100%A	75%A 25%F	50%A 50%F		
	$T_5$	100%A	100%A	100%A	100%A	75%A 25%P	50%A 50%P	37.5%A 37.5%P 25%F	25%A 25%P 50%F			
	$T_4$	100%A	100%A	100%A	100%A	50%A 50%P	100%P	75%P 25%F	50%P 50%F			
	$T_3$	100%A	97.5%A 2.5%B	87.5%A 12.5%B	75%A 25%B	37.5%A 50%P 12.5%B	100%P	75%P 25%F	50%P 50%F			
	$T_2$	97.5%A 2.5%B	95%A 5%B	75%A 25%B	50%A 50%B	25%A 50%P 25%B	100%P	75%P 25%F	50%P 50%F			
	$T_1$	47.5%A 2.5%B 50%M	45%A 5%B 50%M	37.5%A 5%B 37.5%M	25%A 50%B 25%M	12.5%A 50%P 25%B 12.5%M	100%P	75%P 25%F	50%P 50%F			
0	2.5%B 97.5%M	5%B 95%M	25%B 75%M	50%B 50%M	25%P 50%B 25%M	100%P	75%P 25%F	50%P 50%F				
		$t_1$	$t_2$	$t_3$	$t_4$	$t_5$	$t_6$	$t_7$	$t_8$			
		Time of cooling, $t_{8/5}$										

Fig. 3. Contents of ferrite, pearlite, bainite, martensite and austenite at some temperature

Heat conductivity coefficients of microconstituents (ferrite, pearlite, bainite, martensite, austenite) at some temperature which is between noticed temperature in Table 3 was estimated by interpolation. Total heat conductivity coefficients of steel at some temperature,  $\nabla$  were estimated by:

$$\lambda_T = (x_f \lambda_{(F+P)\nabla} + x_p \lambda_{(F+P)\nabla} + x_B \lambda_{B\nabla} + x_M \lambda_{M\nabla} + x_A \lambda_{A\nabla}) / 100 \tag{13}$$

where  $x_f$ ,  $x_p$ ,  $x_B$ ,  $x_M$ ,  $x_A$  are contents, and  $\lambda_{(F+P)\nabla}$ ,  $\lambda_{B\nabla}$ ,  $\lambda_{M\nabla}$ ,  $\lambda_{A\nabla}$  are heat conductivity coefficients of ferrite + pearlite, bainite, martensite and austenite at temperature,  $\nabla$ , respectively. Contents

of ferrite, pearlite, bainite, martensite and austenite at some temperature can be estimated using the diagram in the Fig. 3.

Characteristic cooling times in Fig. 3 are equal to:

$$t_1 = t_{M95} \tag{14a}$$

$$t_2 = \exp(\log t_{M95} + 0.25(\log t_{M50} - \log t_{M95})) \tag{14b}$$

$$t_3 = \exp(\log t_{M95} + 0.75(\log t_{M50} - \log t_{M95})) \tag{14c}$$

$$t_4 = \exp(\log t_{M50} + 0.25(\log t_{P100} - \log t_{M50})) \tag{14d}$$

$$t_5 = \exp(\log t_{M50} + 0.75(\log t_{P100} - \log t_{M50})) \tag{14e}$$

$$t_6 = \exp(\log t_{P100} + 0.25(\log t_{P50} - \log t_{P100})) \tag{14f}$$

$$t_7 = \exp(\log t_{P100} + 0.75(\log t_{P50} - \log t_{P100})) \tag{14g}$$

where  $t_{M95}$ ,  $t_{M50}$ ,  $t_{P100}$ ,  $t_{P50}$  are cooling time from 800 to 500°C for characteristic points in *Jominy* specimen with 95% of martensite, 50% of martensite, 100% of pearlite and 50% of pearlite in microstructure, respectively. The times  $t_{M95}$ ,  $t_{M50}$ ,  $t_{P100}$ ,  $t_{P50}$  was estimated by the conversion of distance from a quenched end of *Jominy* specimen (*Jominy* distance) of characteristic microstructure composition to cooling time,  $t_{8/5}$  by using both, the relation between cooling time,  $t_{8/5}$  and *Jominy* distance and the *Jominy* hardenability curve. The diagram of *Jominy* distance vs. cooling time,  $t_{8/5}$  is shown in Fig. 2. Cooling time between 800 and 500°C should be estimated by extrapolation if the temperature in specimen point is higher than 500°C.

If hardnesses of characteristic microstructure are known, characteristic *Jominy* distance can be found out using the *Jominy* test results. Hardness of characteristic steel microstructure was calculated by equations (15) shown in Table 4.

Table 4. Hardness of characteristic steel microstructure

Microstructure	Hardness
95% martensite + 5% bainite	$HRC_{M95} = 0.93HRC_{max}$ <span style="float:right">(15a)</span>
50% martensite + 50% bainite	$HRC_{M50} = 0.73HRC_{max}$ <span style="float:right">(15b)</span>
100% pearlite	$HV_{P100} = 0.2308HV_{max} + 100$ <span style="float:right">(15c)</span>
50% pearlite + 50% ferrite	$HV_{P50} = 0.1504HV_{max} + 100$ <span style="float:right">(15d)</span>

Characteristic temperatures in diagram shown in Fig. 3 are equal to:

$$T_1 = M_s - 0.75(M_s - M_f) \tag{16a}$$

$$T_2 = M_s - 0.25(M_s - M_f) \tag{16b}$$

$$T_3 = B_s - 0.75(B_s - M_s) \tag{16c}$$

$$T_4 = B_s - 0.25(B_s - M_s) \tag{16d}$$

$$T_5 = A_1 - 0.75(A_1 - B_s) \tag{16e}$$

$$T_6 = A_1 - 0.25(A_1 - B_s) \tag{16f}$$

$$T_7 = A_3 - 0.75(A_3 - A_1) \tag{16g}$$

$$T_8 = A_3 - 0.25(A_3 - A_1) \tag{16h}$$

where  $M_s$  is temperature of start of martensitic transformation;  $M_f$  is temperature of finish of martensitic transformation;  $B_s$  is temperature of start of bainitic transformation;  $A_1$  is equilibrium temperature of eutectoid transformation;  $A_3$  is equilibrium temperature at which transformation of austenite to ferrite begins.

Between critical temperatures  $A_3$ ,  $B_s$ ,  $M_s$  and  $M_f$  of austenite decomposition and hardenability properties, regression relations are established:

$$A_3 = 862 - 0.04(\text{HRC}_{\max} - 20)^2 - \frac{6E_d}{\text{HRC}_{\max} - 20} \tag{17a}$$

$$B_s = 586 - 0.02(\text{HRC}_{\max} - 20)^2 - \frac{30.6E_d}{\text{HRC}_{\max} - 20} \tag{17b}$$

$$M_s = 502 - 0.09(\text{HRC}_{\max} - 20)^2 - \frac{9E_d}{\text{HRC}_{\max} - 20} \tag{17c}$$

$$M_f = 502 - 0.2(\text{HRC}_{\max} - 20)^2 - \frac{9E_d}{\text{HRC}_{\max} - 20} \tag{17d}$$

It was accepted that equilibrium temperature of eutectoid transformation  $A_1$  is equal to 721°C.

### 4. Application example

The model was experimentally tested for the steel specimen with complex form made of steel EN 37Cr4. Geometry of steel specimen is shown in Fig. 4. The chemical composition of investigated steel specimen is: 0.36% C, 0.26% Si, 0.75% Mn, 0.012% S, 0.016% S, 1.05% Cr. *Jominy* test results of the

investigated steel are shown in Table 5. The specimen was quenched from 850°C for 45 min/oil with *Grossmann* severity of quenching  $H=0.35$ .

The distribution of hardness of the quenched steel specimen is shown in Fig. 5. Hardness distribution of the quenched steel specimen is calculated using the computer software BS-QUENCHING. Numerically and experimentally estimated hardness HRC in critical locations 1-4 (Figs. 4 and 5) of the quenched steel specimen are shown in Table 6. A difference between experimentally and numerically estimated hardness has been negligible (Table 6).

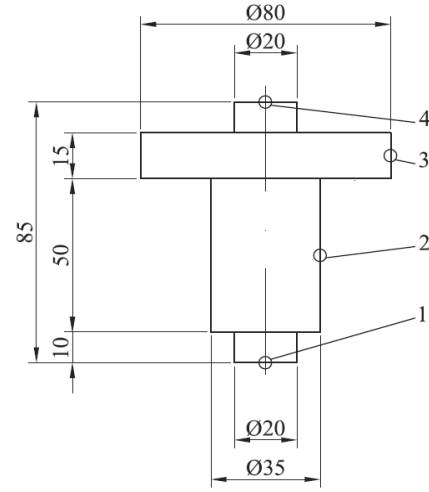


Fig. 4. Geometry of steel specimen

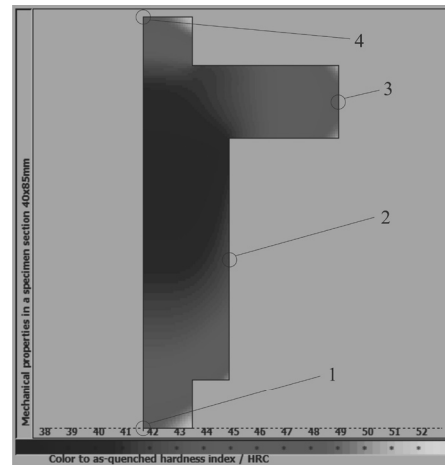


Fig. 5. Hardness distribution in the quenched steel specimen

Table 5.

*Jominy* test results of steel EN 37Cr4

<i>Jominy</i> distance/mm	1.5	3	5	7	11	15	20	25	30	40	50
Hardness HRC	55	55	53	51	44	39	34	31	30	28	27

Table 6.  
Numerically and experimentally estimated hardness in critical locations of quenched steel specimen

Critical location in Fig. 5	Hardness HRC	
	Numerically	Experimentally
1	49	46
2	42	44
3	48	48
4	49	47

## 5. Conclusion

Accuracy of mathematical modelling of steel quenching directly depends on correctness of input variables applied in model. Variable has to be calibrated if it is accepted from literatures. Moreover, all of the variables applied in model should be calibrated, or indirectly estimated based on experiment by some of inversion method. Numerical simulation of quenching, with application of calibrated heat transfer data, is a generalized way of simulation and largely applicable in design offices.

In proposed method of evaluation of input data in mathematical model of quenching density and specific heat capacity of steel have been accepted from literature. Heat transfer coefficient and heat conductivity coefficient have been successfully calibrated by using *Crafts-Lamont* diagrams.

Moreover, the mathematical model of steel quenching has been developed to predict the hardness distribution in a specimen with complex geometry. The model is based on the finite volume method. The numerical simulation of quenching is consisted of numerical simulation of transient temperature field change of cooling process and of numerical simulation of hardening. Hardness in specimen points was calculated by the conversion of calculated time of cooling from 800 to 500°C e to hardness. The established mathematical model was applied in computer simulation of hardness distribution in steel shaft. It can be concluded, that by proposed method hardness in quenched steel specimen can be successfully calculated.

## References

- [1] E. Just, Verguten-Werkstoffbeeinflussung durch harten und anlassen, VDI-Bericht 256 (1976) 124-140.
- [2] L.A. Dobrzański, S. Malara, J. Trzaska, Project of neural network for steel grade selection with the assumed CCT diagram, Journal of Achievements in Materials and Manufacturing Engineering 27/2 (2008) 155-158.
- [3] W. Sitek, J. Trzaska, Hybrid modelling methods in materials science - selected examples, Journal of Achievements in Materials and Manufacturing Engineering 54/1 (2012) 93-102.
- [4] W. Sitek, Employment of rough data for modelling of materials properties, Journal of Achievements in Materials and Manufacturing Engineering 21/2 (2007) 65-68.
- [5] J. Trzaska, A. Jagiełło, L.A. Dobrzański, The calculation of CCT diagrams for engineering steels, Archives of Materials Science and Engineering 39/1 (2009) 13-20.
- [6] W. Crafts, J. Lamont, Hartbarkeit und Auswahl von Stählen, Springer Verlag, 1954.
- [7] B. Liščić, System for Process Analysis and Hardness Prediction When Quenching Axially-Symmetrical Workpieces of Any Shape in Liquid Quenchants, Materials Science Forum 638-642 (2010) 3966-3974.
- [8] A. Felde, T. Réti, Evaluation of cooling characteristics of quenchants by using inverse heat conduction methods and property prediction, Materials Science Forum 659 (2010) 153-158.
- [9] B. Smoljan, The calibration of the mathematical model of steel quenching, Proceedings of the 5<sup>th</sup> World Seminar on Heat Treatment and Surface Engineering, Isfahan, 1, 1995, 709-715.
- [10] B. Smoljan, Numerical simulation of as-quenched hardness in a steel specimen of complex form, Communications in Numerical Methods in Engineering 14/1 (1998) 277-285.
- [11] S. Patankar, Numerical heat transfer and fluid flow, McGraw Hill Book Company, New York, 1980, 60.
- [12] H. Bhadeshia, Material factors, Handbook of residual stress and deformation of steel, ASM International, 2002.
- [13] A. Rose, F. Wever, Atlas zur Wärmebehandlung der Stähle, Verlag Stahleisen, Düsseldorf, 1954.